IEEE Access
Multidisciplinary | Rapid Review | Open Access Journal

Received 4 April 2023, accepted 14 April 2023, date of publication 17 April 2023, date of current version 21 April 2023.

Digital Object Identifier 10.1109/ACCESS.2023.3267972

RESEARCH ARTICLE

Particle Swarm Optimization of Resonant Sonic Crystals Noise Barriers

DAVID RAMÍREZ-SOLANA[1,2], JAVIER REDONDO[2], AGOSTINO MARCELLO MANGINI[1], (Senior Member, IEEE), AND MARIA PIA FANTI[1], (Fellow, IEEE)

[1]Department of Electrical and Information Engineering, Polytechnic University of Bari, 70125 Bari, Italy
[2]Research Institute for the Integrated Management of Coastal Zones, Polytechnic University of Valencia, 46730 Gandia, Spain

Corresponding author: David Ramírez-Solana (david.ramirezsolana@poliba.it)

This work was supported in part by the Spanish "Ministerio de Ciencia e Innovación" and "Agencia Estatal de Investigación" of Spain through project MCIN/AEI/10.13039/501100011033 under Grant PID2021-124908NB-I00, and in part by the European Regional Development Fund (ERDF) A way of making Europe.

ABSTRACT The study of technological materials made by meticulously arranging acoustic elements has received a lot of attention over the past three decades with the goal of generating improved acoustic properties, often going beyond the behavior of materials found in nature. These are frequently referred to as acoustic metamaterials, and because of the way wave propagation phenomena is managed, they exhibit unusual properties. Improvements in noise mitigation techniques of acoustic systems based on metamaterials principles have been made effectively and precisely using combined or hybrid numerical methods and improved numerical formulations. These noise mitigation properties should be optimized by modifying topology and inner elements properties, which requires a huge search space. This work focuses on metamaterials called sonic crystals with Helmholtz resonators, and its innovative insulation properties as noise barriers are optimized with the Particle Swarm Optimization (PSO). This evolutionary algorithm provides a mono objective solution for the multi-dimensional search space inspired in animal behavior looking for food and communicating between each other. In order to assess the results obtained by the proposed approach, the presented PSO algorithm is compared with a Genetic Algorithm (GA): the results show that the PSO algorithm provides a better solution that pursues the objective of satisfying the acoustic comfort without exceeding the imposed practical constraints.

INDEX TERMS Acoustic metamaterials, noise barriers, particle swarm optimization, sonic crystals.

I. INTRODUCTION

The manipulation and control of wave propagation is a fundamentally interesting subject, at the basis of several applications in various fields of science and technology. Localization and concentration of the wave energy, also known as local enhancement of the wave energy, is a crucial aspect of wave manipulation. Artificial compounds, particularly artificial crystals, are showing promise as devices for modifying wave propagation [1], [2]. Sonic crystals (SCs) are artificial periodic materials that are used in the study of sound waves and are structurally like photonic crystals used in the study of optics. They are synthetic infills from a periodic distribution of elements or scatterers with different properties (e.g., elasticity and density) from the host medium, in case of SCs, the host medium is air. This causes a periodic variation of the medium's acoustic characteristics at the wavelength scale. Due to their unusual dispersive qualities, these materials have a strong ability to manipulate the propagation of sound waves.

The sound waves manipulation has so far been used to illustrate a helpful effect in the noise environment field, such as the development of Band Gaps (BGs), frequency ranges where the waves cannot propagate [3].

Novel devices including acoustic diffusers, waveguides, and noise barriers have been developed and proven using these wave propagation properties [4], [5].

The associate editor coordinating the review of this manuscript and approving it for publication was Guido Lombardi.

The concept of using these periodic acoustic media as attenuation devices is, for example, an alternative to noise barriers based on the ability of manipulating the sound by use of SCs [6]. However, the size and position of these BGs, depend on several variables, including the arrangement of the scatterers or the incidence angle of the wave. Therefore, the simple existence of multiple scattering BGs from an acoustical perspective is insufficient to use SCs as noise barriers. The main reason is because traditional noise barriers are insulating from 100 Hz until 5 kHz, covering the full traffic spectrum and SCs only have big insulation in the BGs. Hence, the global insulation value would be very low. To address these issues, certain methods to improve the acoustical characteristics of SCs have been recently explored, like the addition of Helmholtz resonators embedded in the scatter's topology [7], [8]. By adding the Helmholtz resonators, new insulation ranges can appear considering the whole frequency range (100 Hz – 5kHz) and consequently the global insulation value will increase.

Additionally, the investigation of SCs manufactured with scatterers having resonant effects has been conducted, with promising results, particularly at frequencies lower than the BGs. Recently, several works combined these effects to improve the SCs' applications as noise barriers [9], [10].

On the other hand, numerical simulation techniques, as finite elements method (FEM), are useful engineering tools in the current research of development of acoustic materials and assembled systems.

As a result, several acoustic issues have come out where numerical modeling has been crucial in improving the acoustic properties of various acoustic metamaterials and systems within the context of a wide scope of applications such as acoustic black holes [11], resonant phononic crystals with acoustic imaging properties [12], transmission characteristics of H-type metamaterials [13] or coupled resonant materials that can reduce noise [14].

The development of numerical algorithms to assess the acoustic performance of these devices is crucial to accurately predict the acoustic performance of new noise barriers before their construction. Hence, these simulation techniques have aided the advancement of acoustics technology and the creation of novel devices, such sonic crystals noise barriers (SCNB).

Furthermore, numerical simulation techniques combined with optimization algorithms are efficient design procedure for obtaining improved acoustic performance and new functionalities of the devices [15]. In the specific case of SCNB, evolutionary genetic algorithms have been applied to optimize the acoustic devices, through numerical models and by modifying the properties of the structure [16], [17]. In these works, multi-objective optimization approaches of SCNB are used by selecting only one or two input parameters. If new input parameters are added in the optimization model, the search space turns into extremely huge and complex, so the need of avoiding local maximum/minimum solutions becomes a main handicap to deal with.

In this paper we overcome the previous drawbacks, by proposing a new technique to optimize the parameters of SCNB. More precisely, the SCNB is described by 2D simulation models and the best insulation levels of the barriers are obtained by applying a Particle Swarm Optimization (PSO) algorithm [18], [19].

Note that the PSO algorithms have been applied to several acoustics' cases, such as acoustic radiation [19], porous materials [20], ultrasonic transducers [21], acoustic filters [22], room acoustics [23], all of them having an enormous ranges for the search space, in the optimization process.

The numerical technique used for modelling the system and assessing the performance of each possible solution is the Finite Elements (FE) simulations.

In particular, this paper focuses on a key element of the SCNB: the optimization of the scatterer's topology and the periodicity of the metamaterial that depends on the lattice constant distance.

To assess the results obtained by the proposed approach, the presented PSO algorithm is compared with GA.

PSO and GA are both popular metaheuristic optimization algorithms used to solve complex optimization problems. It is important to note that the performance of PSO and GA can depend on the specific problem being solved [24], [25], [26]. In the considered case, the following advantages of PSO over GA are deduced by the simulation analysis and study.

1. **Less prone to getting stuck in local optima:** We verified that in the considered problem PSO is less likely to get stuck in local optima than GA because it uses velocity and position to update the particles' position in the search space. This allows PSO to escape from local optima and continue exploring the search space. On the other hand, the search space of the presented problem has large 4-dimensional range of possible combinations. All these combinations can bring very different fitness values even modifying only one of the physical parameters to optimize.
2. **Smaller computational effort:** In the performed experiments we verified that PSO converged to the optimal solution more quickly than GA. This is because PSO combines global and local search mechanisms which allow exploring the search space more efficiently than GA.
3. **Robustness:** PSO resulted more robust than GA because it does not require a fitness function that is differentiable or continuous. PSO can handle noisy and discontinuous fitness functions as the noise barriers global insulation value presented in this study.

The results show that the PSO algorithm provides a good solution that pursues the objective of satisfying the acoustic comfort without exceeding some imposed practical constraints.

The paper is organized as follows. Section II presents the employed methodology and Section III specifies the case study of SCNB optimization module. Moreover, Section IV

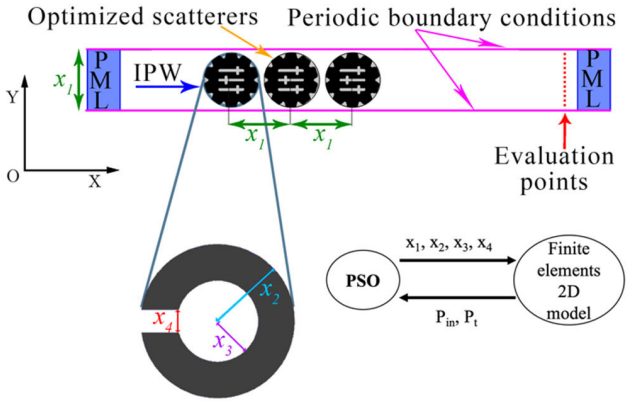

FIGURE 1. 2D Finite elements model of periodic sonic crystal noise barrier. 3 rows of scatterers to be optimized and the distance between them too with the PSO algorithm.

presents the results and Section V discusses the comparison with GA and random values. Finally, Section VI summarizes the conclusions and the future works.

II. METHODOLOGY

The tools and procedures to optimize the SCNB are presented in this section. First, the specifications of the model that should be optimized is described, second the applied optimization algorithm is presented, third the GA and random search used to enlighten and compare the obtained benefits are explained.

A. FINITE ELEMENTS 2D MODEL

In this subsection we describe the FE 2D model of the SCNB that needs to be optimized. The aim is to obtain a precise simulation model requiring low computational cost to apply the optimization process that calls for several iterations.

Moreover, an exact estimation of the acoustic performance of the various proposed designs is requested. In addition, since the SCNB are typically built throughout extremely long extensions of kilometers in the borders of highways or railroads, the model showed in Fig. 1 represents a semi-infinite width barrier. This barrier receives the sound coming from the left part of the model and the remaining acoustic pressure that pass through the noise mitigation device is evaluated at the right part of the model at the red points.

To eliminate unwanted reflections (free field condition), Perfectly Matched Layers (PMLs) are positioned at the vertical contours (left and right), and the incident plane wave (IPW) travels from left to right [27]. The horizontal contours are periodic conditions that repeat the model in the Y axis, the evaluation points are placed one meter away from the edge of the last scatter. These values are averaged to cover a more general behavior in the performance zone of the barrier.

The four physical parameters that define the topology of the scatterers and the periodicity of the SCNB are represented in Fig. 1:

- the lattice constant x_1 that is the periodicity of the metamaterial, i.e., the separation between rows and columns of the center of the scatterers .
- the external radius of the cylindrical scatter x_2;
- the internal radius of the cylindrical scatter x_3;
- the width of the mouth of the Helmholtz resonator embedded in the scatter x_4.

We remark that by using the described model, the computational cost of the result of each simulation is varying depending on the topology and how the elements of the domain are adapting to the shape with the FE mesh.

B. THE PARTICLE SWARM OPTIMIZATION

The PSO is part of the evolutionary algorithm's family and is based on the animal behavior. The original version of the algorithm tried to simulate the social behavior of the animals to model their fly, changing of position and researching the global best position. In the PSO algorithm several components, called particles, are placed in the search space of the problem, and each of them evaluates the fitness (or objective) function at its current location. Each particle determines its movement through the search space by combining some aspects of the history of its own current and best positions with those of the nearest members of the swarm. The next iteration takes place after all particles have been moved. The swarm as a whole, like flock of birds foraging for food, moves close to an optimum of the fitness function [28].

Each particle of the swarm is composed of three D-dimensional vectors, where D is the dimension of the search space: the current position $\boldsymbol{X}_j$, the previous best position $\boldsymbol{Xbest}_j$, and the velocity $\boldsymbol{v}_j$. The current position $\boldsymbol{X}_j$, considered as a set of coordinates describing a point in the space, is evaluated as a possible problem solution. If such position results to be better than the previous ones, then its coordinates are stored in the vector $\boldsymbol{Xbest}_j$. The value of the resulted best function is stored in a variable called previous best $pbest_j$, for comparison on the later iterations. The objective of the algorithm is to find better positions and update $\boldsymbol{Xbest}_j$ and $pbest_j$. Moreover, the algorithm iteratively updates the velocity vector $\boldsymbol{v}_j$ and calculates new points by adding the $\boldsymbol{v}_j$ coordinates to $\boldsymbol{X}_j$.

A version of the PSO algorithm can be explained according to the following algorithm steps [29].

PSO Algorithm

1) STEP 1

Initialize a population array of N particles with random positions and velocities on D dimensions in the search space.

2) STEP 2

At the iteration k execute the loop:

1. For each particle, evaluate the desired optimization fitness function in D variables by simulating the described FE model.

2. Compare particle's fitness evaluation with its $pbest_j$. If the current value is better than $pbest_j$, than set $pbest_j$ equal to the current value, and $\boldsymbol{X}best_j$ equal to the current location $\boldsymbol{X}_j \in R_+^D$ where R_+ is the set of real positive numbers.
3. Identify the particle in the group of N particles with the best success so far and assign its index to the vector $\boldsymbol{X}gbest$ and variable $gbest_j$.
4. Change the velocity and position of the particle according to the following equations, respectively:

$$\begin{aligned}\boldsymbol{v_j}(k+1) = w \cdot \boldsymbol{v}_j(k) + c_1 \cdot r_1^{(k)} \\ \cdot \left[\boldsymbol{X}best_j(k) - \boldsymbol{X_j}(k)\right] \\ + c_2 \cdot r_2^{(k)} \cdot \left[\boldsymbol{X}gbest_j(k) - \boldsymbol{X_j}(k)\right] \quad (1)\end{aligned}$$

$$\boldsymbol{X}_j(k+1) = \boldsymbol{X}_j(k) + \boldsymbol{v}_j(k+1) \quad (2)$$

5. If a stop criterion is met, then exit loop.

In the velocity equation (1) the w factor is called inertia weight. It was introduced in [30] to reduce the effect of the maximum velocity, affecting the impact of $\boldsymbol{v}(k)$ on $\boldsymbol{v}(k+1)$. In addition, r_1 and r_2 are random numbers in the range [0,1], c_1 and c_2 are positive constants, called acceleration coefficients, which are responsible for appropriately weighting both the cognitive and social components. Indeed, the velocity of particles drives the optimization process through the cognitive component, based on particle's historical information, and the social component with information about the best solution found by the swarm.

Some parameters must be appropriately chosen, depending on the problem to be solved, to guarantee the algorithm convergence. The number of particles is typically chosen between 10 and 50. But depending on the search space dimension, it can be necessary to increase the number of particles to have a wider exploration. The maximum velocity of each parameter to optimize is given by the following equation:

$$\boldsymbol{v}_{max} = h * \frac{(\boldsymbol{X}_{max} - \boldsymbol{X}_{min})}{2}, \quad (3)$$

where $0 \leq h \leq 1$ is the clamping factor, and $\boldsymbol{X}_{max}^T = [x_{1max}, x_{2max}, x_{3max}, x_{4max}]$ and $\boldsymbol{X}_{min}^T = [x_{1min}, x_{2min}, x_{3min}, x_{4min}]$ are the vectors including the maximum and minimum values that each element of $\boldsymbol{X}_j$ can be settled in the optimization process, respectively. Note that maximum the velocity of each particle is limited by the range $[-\boldsymbol{v}_{max}, +\boldsymbol{v}_{max}]$.

Generally, the inertia weight w at iteration k is given by the following equation:

$$w(k) = w_{min} + \frac{(itr_{max} - k) \cdot (w_{max} - w_{min})}{(itr_{max} - 1)} \quad (4)$$

where itr_{max} is the maximum number of iterations of the algorithm and k is the current iteration. Typically, $itr_{max} = 10$ and $w(k)$ decrease in the interval [0.9, 0.4], by guaranteeing the equilibrium between exploration and exploitation.

The following relationship between c_1, c_2 and w guarantees the PSO algorithm convergence [30]:

$$w > \frac{1}{2}(c_1 + c_2) - 1 \quad (5)$$

In particular, choosing $w = 0.7298, c_1 = c_2 = 1.49618$ provides good convergent behavior [31].

C. GA AND RANDOM SEARCH

With the goal of having a more global vision of the case study, two more methodologies are compared with the PSO in the SCNB model, i.e., GA and Random search.

As it has been said in the introduction, GA has been already used to optimize SCNB without Helmholtz resonators, so in this case the model and the function to optimize would be the same as the PSO case to compare the optimization process and results.

Concerning the random search, the number of the simulations to be evaluated is chosen equal to the number of simulations needed to find the convergence in the PSO best Fitness value. So, we select with uniform probability the components of $\boldsymbol{X}_j$ between the values of the corresponding components of $X_{min}^T = [x_{1min}, x_{2min}, x_{3min}, x_{4min}]$ and $\boldsymbol{X}_{max}^T = [x_{1max}, x_{2max}, x_{3max}, x_{4max}]$.

In a "box and whiskers" plot, the results of random simulations and the corresponding fitness function values are represented. More specifically, the boxplot shows with the red line the median of all values, and the blue limits of the box are the upper and lower quartiles, respectively. The red crosses are the outliners of the found minimum and maximum values.

III. CASE STUDY: THE SCNB OPTIMIZATION MODULE APPLYING PSO ALGORITHM

In this section we present the SCNB optimization module. In detail we consider a specified application of the optimization that is applied to determine the optimal topology of the scatterers and periodicity of the 2D model showed in Fig. 1. The aim is guaranteeing the biggest attenuation possible in the frequency range [100-5000 Hz] included in the European Standards [32], [33], one of the main objectives of the noise barriers. The problem is solved by using the PSO that turns out to be an effective tool to optimize this type of problems with such a difficult search space. Indeed, the PSO algorithm has the properties of fast execution, not complex implementation, parallel behavior, and no need to have the problem optimization to be differentiable [22].

A. FITNESS FUNCTION

The fitness function $gbest$ to optimize is a single value to express how good is the barrier insulating noise. The European Standards EN 1793-3 [32] and EN 1793-6 [33] define the calculation proceeding of the single-number rating of the airborne sound insulation for road traffic (sound

TABLE 1. Normalized traffic noise spectrum.

m	Central frequency [Hz]	L_i [dB]
1	100	-20
2	125	-20
3	160	-18
4	200	-16
5	250	-15
6	315	-14
7	400	-13
8	500	-12
9	630	-11
10	800	-9
11	1000	-8
12	1250	-9
13	1600	-10
14	2000	-11
15	2500	-13
16	3150	-15
17	4000	-16
18	5000	-18

insulation index DL_{SI}) as follows:

$$DL_{SI} = -10 \cdot \log\left(\frac{\sum_{i=m}^{18} 10^{0,1\cdot \boldsymbol{L}_i} \cdot 10^{-0,1\cdot \boldsymbol{SI}_i}}{\sum_{i=m}^{18} 10^{0,1\cdot \boldsymbol{L}_i}}\right) \text{dBA} \quad (6)$$

where m is the number of the third octave band frequency spectrum and L_i is the dB-value of the i-th third-octave band of the traffic noise spectrum, represented in Table 1, according to EN 1793-3 [32].

$\boldsymbol{SI}_i$ is the value in dB of the i-th third-octave band of the sound insulation spectrum which is calculated in the FEM Model at the evaluation points:

$$SI = 20 \cdot log_{10}\left|\frac{\mathrm{P_{in}}}{\mathrm{P_t}}\right| \text{dB} \quad (7)$$

where $\mathrm{P_{in}}$ is the value of the incident effective pressure without the barrier and $\mathrm{P_t}$ is the value of the effective pressure transmitted with the barrier placed. Both pressures are obtained at the same evaluation points showed in Fig. 1.

Even if the standards only have the central frequency of each octave band, in the FEM model, the average of 3 frequencies of each octave band has been calculated to achieve a more precise representation of the full frequency spectrum.

The upper and lower bounds of the 4-dimensional search space ($D = 4$) to optimize are limited to create as maximum, 1 m length of noise barrier and only 3-rows of scatterers, which means according to the external radius and the lattice constant that $2^*(x_1 + x_2) = 1$. Hence, we impose $\boldsymbol{X}^T_{max} = [0.3900, 0.1755, 0.1667, 0.3301]$ and $\boldsymbol{X}^T_{min} = [0.1000, 0.0300, 0.0015, 0.0001]$.

In doing this, the models are more realistic approaches to already existing conventional noise barriers length.

B. PROCESS OF THE OPTIMIZATION

The PSO algorithm is described by the following pseudocode that implements the steps described in Section II-B.

Particle Swarm Optimization Algorithm for SCNB

1st phase: Initialize particles with k = 0

Set the configuration coefficients N, itr_{max}, c_1, c_2, w_{min}, w_{max}
Set search space ($D = 4$), upper and lower bounds of $\boldsymbol{X}$
Set ($k = 0$), ($DL_{SI\boldsymbol{gbest}} = 0$) and N particles: p_j= ($\boldsymbol{X}_j$, $\boldsymbol{X}best_j$, $\boldsymbol{v}_j$)
for j = 1: N do
  Set random values of $\boldsymbol{X}_j = [x_{1j}, x_{2j}, x_{3j}, x_{4j}]^{\mathrm{T}}$
  p_j = ($\boldsymbol{X}_j$, (0,0,0,0),(0,0,0,0))
end for

2nd phase: Evaluate Fitness values

$k = k + 1$ until $k = itr_{max}$
for j = 1: N
  for i = m = 1: 18
    Simulate the Finite Elements Model with $\boldsymbol{X}_j$
    Obtain $\mathrm{P_t}$ and $\mathrm{P_{in}}$
    Calculate $\boldsymbol{SI}_i$
  end for
  Calculate DL_{SIj}
end for

3rd phase: Analysis

for j = 1 : N
  if $DL_{SIj} > DL_{SI\boldsymbol{pbest}j}$
    $\boldsymbol{X}best_j = \boldsymbol{X}_j$
  end if
end for
$DL_{SI\boldsymbol{gbest}}$ =max ($DL_{SI\boldsymbol{gbest}}$, $\max_{\mathrm{j=1:N}}(DL_{SI\boldsymbol{gbest}})$)
$\boldsymbol{X}gbest$ = select $_{\mathrm{j=1:N}}\{p_j that\ DL_{SIj} = DL_{SI\boldsymbol{gbest}j}\}$

4th phase: Swarm updates

for j = 1: N at k iteration
  Calculate inertia $w(k)$ according to equation (4)
  Calculate future velocity $\boldsymbol{v}_j(k+1)$ according to equation (1)
  Calculate future position $\boldsymbol{X}_j(k+1)$ according to equation (2)
  Set p_j = ($\boldsymbol{X}_j(k+1)$, $\boldsymbol{X}best_j$, $\boldsymbol{v}_j(k+1)$)
end for
if $k <$ itr_{max} Go to 2nd phase

5th phase: End of the process

$\boldsymbol{X}_{optim}$=$\boldsymbol{X}gbest$
Return $\boldsymbol{X}_{optim}$
end of optimization process
EXIT

The optimization process is carried out according to the block diagram shown in Fig. 2. Multiple simulations have been run on the extensive 4-dimensional search space, seeking for the optimal PSO coefficients and varying population sizes. It is important to remark that in this iterative procedure, each particle $\boldsymbol{X}_j = [x_{1j}, x_{2j}, x_{3j}, x_{4j}]^{\mathrm{T}}$ requires a new model set up modification of the one described in Section II-A.

IV. RESULTS

In this section the results of the PSO application are presented, together with the parameters that assure the best value of the fitness function and the behavior of the optimized SCNB.

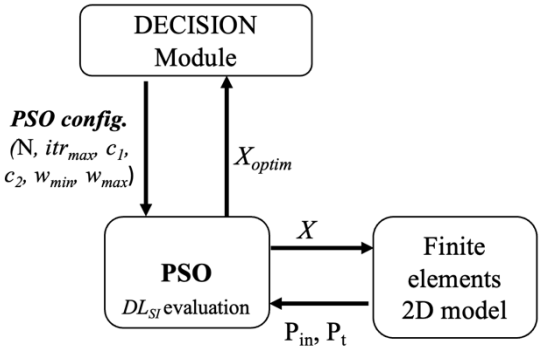

FIGURE 2. Block diagram of the PSO process.

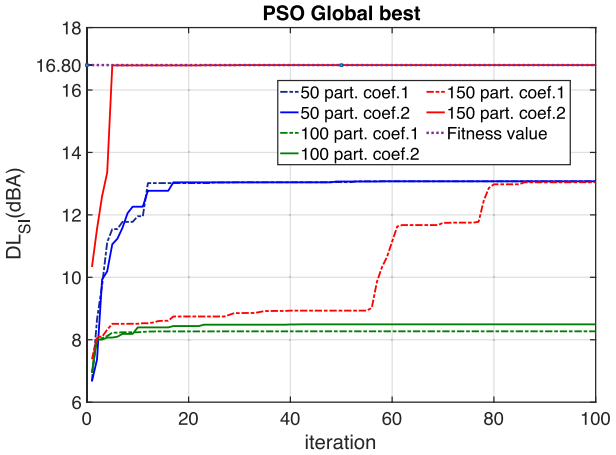

FIGURE 3. Particle Swarm optimization with 100 iterations and different populations and coefficients.

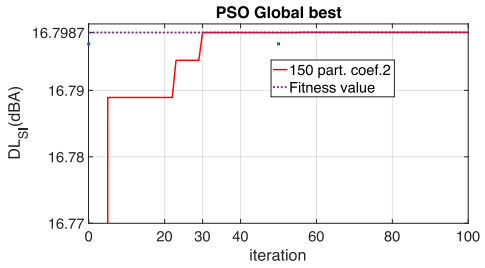

FIGURE 4. Convergence detail for the best configuration of coefficients and population.

A. ACCELERATION COEFFICIENTS

Two different configurations of coefficients w, c_1 and c_2 have been chosen to run the optimization. The term c_1 stands for the cognitive component and depicts the tendency of the particles to go to their best positions, while the coefficient c_2 is the social component and depicts the attraction of the particle toward the location connected to the overall best value.

The first configuration is called ***coef.1*** where $w = 0.7298$, and $c_1 = c_2 = 1.49618$ are settled following the proposal of Eberhart and Shi [31], for a solid and fast convergence.

Moreover, to address the complexity of the 4-dimensional search space, a second parameter configuration is considered for obtaining a wider exploration of the local maximums. Hence, in the second parameter configuration, called ***coef.2***, it holds $w \in [0.4, 0.9]$ (i.e., the value of w decreases starting from $w = 0.9$ at each iteration k according to equation (4)), $c_1 = 1.53$ and $c_2 = 2.03$. In this second case more importance is given to the social behavior of the particles (c_2) rather than the individual component (c_1) [29].

The faster convergence obtained with the configuration ***coef.1*** with respect to ***coef.2***, is shown in the results of Fig. 3 in the 100 particles case.

B. PSO COMPUTATIONAL PERFORMANCE

The results obtained by considering different populations (50, 100 and 150) and the two proposed sets of coefficients in the 4-dimentional search space are shown in the Fig. 3. We do not report the results obtained with larger number of populations because we verified that the results do not improve with the number of particles greater than 150.

First, population number is as much important as acceleration coefficients, since bigger populations can follow other particles and stop exploring just because the inertia and coefficients force to do it.

Second, as expected, ***coef.1*** goes into solid convergence results, but falling in local maximums. On the other hand, the ***coef.2*** allows us to obtain a better exploration and a higher maximum is found: the first iterations of 150 particles population give the best value $\boldsymbol{DL_{SI}}$ **of 16.80 dBA** as Fig. 3 illustrates.

Even though the European standards only consider values with two decimals for the DL_{SI}, to model a more precise scatter, values until four decimals are evaluated to find the convergence. In Fig. 4, the meticulous adjustment of the fitness value and its convergence for the best optimization case are represented.

In particular, Fig. 4 shows that the convergence of the Fitness value is found at iteration number 30 with a population of 150 particles, after simulating 4500 different models of the SCNB.

By using the model described in Section II-A, the computational cost of the result of each simulation is varying depending on the topology and how the elements of the domain are adapting to the shape with the FE mesh. Computational time of each simulation varies from 7 seconds to 20 seconds. The MATLAB environment is run in a single-thread mode with a computer MAC-mini equipped by a 3 GHz Intel Core i5 of 6 cores and 8 GB of RAM memory.

C. FITNESS OPTIMIZATION PARAMETERS

Table 2 shows the values that maximize the fitness function and yield a $\boldsymbol{DL_{SI}}$ **value of 16.80 dBA**. The local maximums are always discovered with the same shape topology as the global optimal solution, but with a different lattice constant x_1. This makes the lattice constant be the dominant parameter and the most crucial one to set in the SCNB. The scatter's

TABLE 2. Optimal parameters X_{optim} that maximize the DL_{SI}.

Parameter	Name	Value
x_1	Lattice constant (m)	0.3121
x_2	External radio (m)	0.1404
x_3	Internal radio (m)	0.1334
x_4	Mouth width (m)	0.2642
gbest	**DL_{SI} - single-number rating of the airborne sound insulation for road traffic (dBA)**	**16.80**

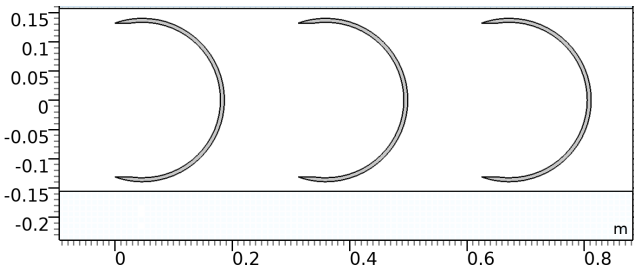

FIGURE 5. Detail of the 2D model with the optimized SCNB.

parameters (external and internal radius and mouth width) discover the global maximum by setting them to values just below the upper bound's limits.

The periodic metamaterial's exterior radius is the 45% of the lattice constant value, the mouth of the resonator is 99% of the internal radius value, and the internal radius is 95% of the external radius.

The final 2D model of the SCNB with the optimized parameters is represented in Fig. 5 with a length of 0.81m. That size will make it easier to place it in the highways and other noisy environments where the barrier will mitigate noise traffic spectrum. It is simple to see from the shape how large the inner resonant air mass is and how thin the surface of the C-shape scatterers is. The tiny amount of stiff material required in the future will reduce the costs associated with fabricating this wide-spectrum SCNB using 3D printing technology.

D. THE OPTIMIZED SCNB BEHAVIOR

Figure 6 shows the outcome of the optimized SCNB sound insulation SI (equation 7) at 1m away from the last scatter in a Finite Elements simulation using the 2D model seen in Fig.1. The Helmholtz resonator's wide-open mouth, which is embedded in the scatter, enhances the barrier's low-frequency insulation, particularly in the range of 150–550 Hz, which is a recurring problem with complex real solutions for thin noise barriers (less than 1m of length). In addition, Fig. 6 represents the third-octave band average of the spectrum that is used in equation (6) to evaluate the Fitness function. Also, those central frequencies showed in Table 1 are the ones considered in the European Standards EN 1793-3 [32] and EN 1793-6 [33]: the average of values (in red in Fig. 6) of

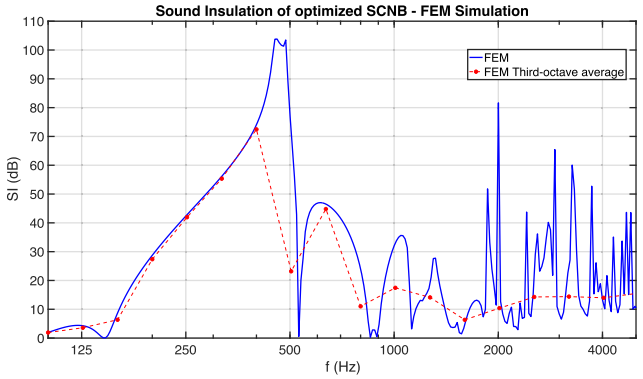

FIGURE 6. Sound Insulation (SI) of the SCNB FEM simulation that maximizes the fitness function.

TABLE 3. Categories of noise barrier according to their airborne sound insulation.

Category	Single Number Rating, DL_{SI} (dBA)
D0	Not determined
D1	<16
D2	**16 to 27**
D3	28 to 36
D4	>36

each frequency band helps to avoid the uneven behavior at high frequencies (more than 1000 Hz).

To show the noise maximum and minimum levels spatially distributed in the SCNB, Fig.7a displays a Sound Pressure Level (dB) map of the model. In that representation it can be clearly seen the attenuation of approximately 90 dB in Fig. 7a at the shadow zone of the barrier, more specifically at the frequency of the maximum in the Insertion Loss spectrum. Figure 6 shows the maximum sound insulation at 486 Hz which reports a value of 103.5 dB.

The first BG frequency produced physical structure of the barrier, and more specifically depending on the lattice constant occurs at $F_{Bragg} = 549$ Hz, and Fig. 7b illustrates a 40 dB attenuation level at that frequency. The two noise-control mechanisms in this SCNB model are multiple scattering and Helmholtz resonances, although absorbent materials frequently utilized as a third to improve attenuation of higher frequencies [34]. Above 2 kHz, the harmonics of the BG and Helmholtz resonance frequencies produce enormous attenuation peaks with narrow frequency ranges, which increase the average attenuation of the SCNB, as seen in Fig. 6.

The optimized barrier is assigned a D2 category in Table 3 of the European Standard Classification [35], rounding $DL_{SI} = 16.80$ dBA to 17 dBA.

V. DISCUSSION AND COMPARISON

In this section, the results obtained by the PSO optimizations are compared with two optimization strategies: the GA and the random simulations. With the purpose of comparing the

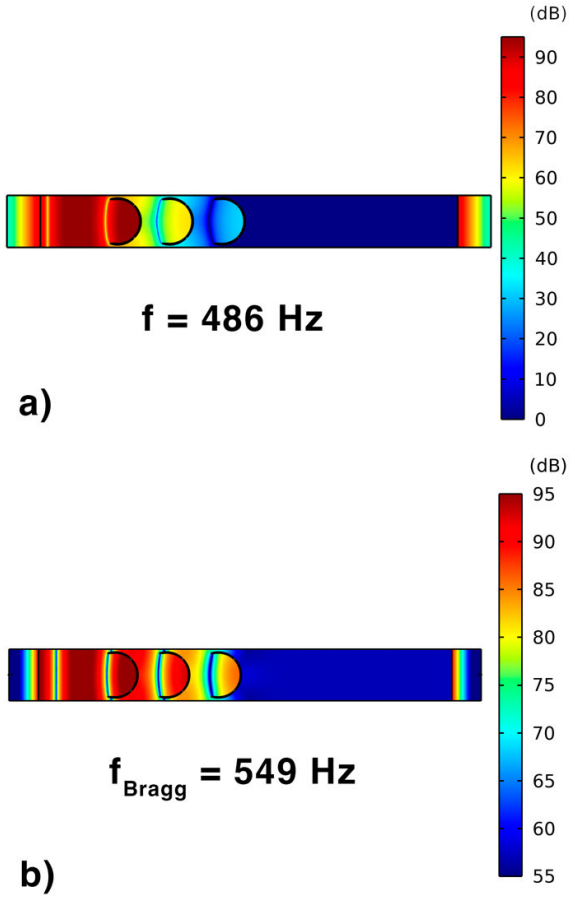

FIGURE 7. Maps of Sound Pressure Level (dB) of the FEM model at maximum attenuation frequency (a) and Bragg's frequency (b).

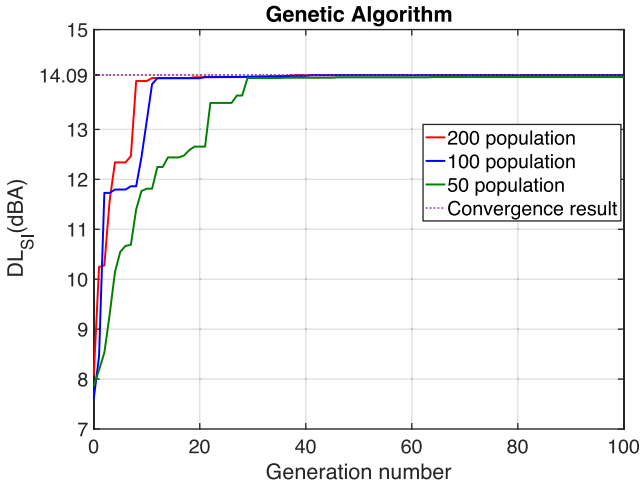

FIGURE 8. Genetic algorithm with 100 generation and different population sizes to optimize the SCNB model.

results with the methodology usually applied in these noise barriers optimizations with acoustic metamaterials, a benchmark with a GA is made [36]. In these optimizations, the diagram process is like the diagram shown in Fig. 2 but instead of updating the position of the particles, the GA changes the gens of the next generation of the population.

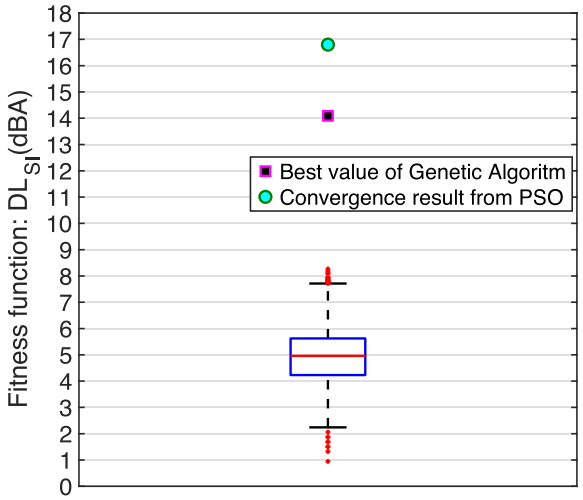

FIGURE 9. Box and whiskers plot of 4500 random simulations of the SCNB model and the best values of PSO and Genetic algorithm optimizations.

The algorithm parameters for all the population cases are the following: mutation probability equal to 0.1, crossover probability is 0.9, and 0 value of linear crossover. This configuration is established by default in the GA for a best behavior in almost all cases. In Fig. 8, the performance of the optimization is represented, giving a convergence result of $DL_{SI} = 14.0861$ dBA, rounded to 14.09 dBA. One of the best properties of the PSO algorithm is its ability to avoid local maximums/minimums. Indeed, the results obtained by the GA proved that in the search space there is a strong local maximum located of 14.09 dBA that the PSO is capable to overpass, giving a result almost 3 dBA greater than that value.

In order to have a more comprehensive understanding of the case study, a third method is compared to this SCNB model. In particular, the values of the SCNB model parameters are randomly selected in the interval $[\boldsymbol{X}_{min}, \boldsymbol{X}_{max}]$ with uniform probability obtaining 4500 random SCNB models.

Figure 9 reports the best values of the fitness function (6) obtained by the GA (with 200 population and 100 generations), the PSO (after 4500 simulations and 150 particles at 30^{th} iteration), and the random methodology, respectively. In particular, the random results are plotted by a ''box and whiskers''. As it is clearly seen, both optimization algorithms (GA and PSO) have improved the random results. Also, they have brought values nearly the double of the Fitness function, with 14.09 dBA in the GA case and 16.80 dBA in the PSO case.

VI. CONCLUSION

This paper's main research objective was to optimize a SCNB model, which is typically syntonized to attenuate a few chosen frequency ranges and making it cover the entire spectrum of traffic noise. Without the addition of absorbent material, as wide-band sonic crystal existents in literature were prone

to do, the PSO algorithm has brought about a novel topology for scatterers. Also, the thin geometry of the final scatterers will help to 3D printed or built it with low costs. This study has demonstrated how metamaterials like Sonic crystals can have a strong performance as a noise barrier competing with the traditional barriers attenuation levels and tested with the European Standards by combining a PSO with FEM simulations in a periodic model. In particular, the single-number rating of the airborne sound insulation for road traffic is $DL_{SI} = 17$ dBA in accordance with European Standards EN 1793-6 and EN 1793-3. Regardless of the length of this optimized SCNB is shorter than 1m (0.81 m), which makes it easy to install it along highway edges, and the Helmholtz resonances help it to achieve a very high level of low-frequency noise insulation. According to the classification of European standards, the sound insulation single value (DL_{SI}) of 17 dBA is a D2 category barrier.

In the future research, a comparison with other numerical methods as Finite Difference Time Domain (FDTD) or the experimental validation of the results will be considered.

REFERENCES

[1] M. M. Sigalas and E. N. Economou, "Elastic and acoustic wave band structure," *J. Sound Vibrat.*, vol. 158, no. 2, pp. 377–382, Oct. 1992.

[2] M. S. Kushwaha, P. Halevi, L. Dobrzynski, and B. Djafari-Rouhani, "Acoustic band structure of periodic elastic composites," *Phys. Rev. Lett.*, vol. 71, no. 13, pp. 2022–2025, Sep. 1993.

[3] R. Martínez-Sala, J. Sancho, J. V. Sánchez, V. Gómez, J. Llinares, and F. Meseguer, "Sound attenuation by sculpture," *Nature*, vol. 378, no. 6554, p. 241, Nov. 1995.

[4] J. Redondo, R. Picó, V. J. Sánchez-Morcillo, and W. Woszczyk, "Sound diffusers based on sonic crystals," *J. Acoust. Soc. Amer.*, vol. 134, no. 6, pp. 4412–4417, Dec. 2013.

[5] T. Miyashita, "Sonic crystals and sonic wave-guides," *Meas. Sci. Technol.*, vol. 16, no. 5, pp. R47–R63, Apr. 2005.

[6] J. V. Sanchez-Perez, C. Rubio, R. Martinez-Sala, R. Sanchez-Grandia, and V. Gomez, "Acoustic barriers based on periodic arrays of scatterers," *Appl. Phys. Lett.*, vol. 81, no. 27, pp. 5240–5242, Dec. 2002.

[7] A. B. Movchan and S. Guenneau, "Split-ring resonators and localized modes," *Phys. Rev. B, Condens. Matter*, vol. 70, no. 12, Sep. 2004, Art. no. 125116.

[8] X. Hu, C. T. Chan, and J. Zi, "Two-dimensional sonic crystals with Helmholtz resonators," *Phys. Rev. E, Stat. Phys. Plasmas Fluids Relat. Interdiscip. Top.*, vol. 71, May 2005, Art. no. 055601.

[9] J. Sánchez-Dehesa, V. M. Garcia-Chocano, D. Torrent, F. Cervera, S. Cabrera, and F. Simon, "Noise control by sonic crystal barriers made of recycled materials," *J. Acoust. Soc. Amer.*, vol. 129, no. 3, pp. 1173–1183, Mar. 2011.

[10] A. Krynkin and O. Umnova, "Predictions and measurements of sound transmission through a periodic array of elastic shells in air," *J. Acoust. Soc. Amer.*, vol. 128, pp. 3496–3506, Dec. 2010.

[11] N.-S. Gao, X.-Y. Guo, B.-Z. Cheng, Y.-N. Zhang, Z.-Y. Wei, and H. Hou, "Elastic wave modulation in hollow metamaterial beam with acoustic black hole," *IEEE Access*, vol. 7, pp. 124141–124146, 2019.

[12] S. Tang, R. Wang, and J. Han, "Acoustic focusing imaging characteristics based on double negative locally resonant phononic crystal," *IEEE Access*, vol. 7, pp. 112598–112604, 2019.

[13] S. Tang and J. Han, "Acoustic transmission characteristics based on H-type metamaterials," *IEEE Access*, vol. 7, pp. 96125–96131, 2019.

[14] Z. Wang, Y. Zuo, L. Sun, and X. Zhao, "Noise reduction in tractor cabs using coupled resonance acoustic materials," *IEEE Access*, vol. 10, pp. 32689–32695, 2022.

[15] M. P. Peiró-Torres, M. J. Parrilla Navarro, M. Ferri, J. M. Bravo, J. V. Sánchez-Pérez, and J. Redondo, "Sonic crystals acoustic screens and diffusers," *Appl. Acoust.*, vol. 148, pp. 399–408, May 2019.

[16] J. M. Herrero, S. García-Nieto, X. Blasco, V. Romero-García, J. V. Sánchez-Pérez, and L. M. Garcia-Raffi, "Optimization of sonic crystal attenuation properties by *ev*-MOGA multiobjective evolutionary algorithm," *Struct. Multidisciplinary Optim.*, vol. 39, no. 2, pp. 203–215, Aug. 2009.

[17] V. Romero-García, J. V. Sánchez-Pérez, L. M. García-Raffi, J. M. Herrero, S. García-Nieto, and X. Blasco, "Hole distribution in phononic crystals: Design and optimization," *J. Acoust. Soc. Amer.*, vol. 125, no. 6, pp. 3774–3783, Jun. 2009.

[18] J. Kennedy and R. Eberhart, "Particle swarm optimization," in *Proc. IEEE Int. Conf. Neural Netw.*, Perth, WA, Australia, Aug. 1995, pp. 1942–1948.

[19] J.-Y. Jeon and M. Okuma, "Acoustic radiation optimization using the particle swarm optimization algorithm," *JSME Int. J. Ser. C*, vol. 47, no. 2, pp. 560–567, 2004.

[20] X. Xu and P. Lin, "Parameter identification of sound absorption model of porous materials based on modified particle swarm optimization algorithm," *PLoS ONE*, vol. 16, no. 5, May 2021, Art. no. e0250950.

[21] D. Chen, J. Zhao, C. Fei, D. Li, Y. Zhu, Z. Li, R. Guo, L. Lou, W. Feng, and Y. Yang, "Particle swarm optimization algorithm-based design method for ultrasonic transducers," *Micromachines*, vol. 11, no. 8, p. 715, Jul. 2020.

[22] R. Barbieri, N. Barbieri, and K. F. de Lima, "Some applications of the PSO for optimization of acoustic filters," *Appl. Acoust.*, vol. 89, pp. 62–70, Mar. 2015.

[23] M. Szczepanik, A. Poteralski, J. Ptaszny, and T. Burczyński, "Hybrid particle swarm optimizer and its application in identification of room acoustic properties," in *Proc. Int. Symp. Evol. Comput.*, vol. 7269. Berlin, Germany: Springer, 2012, pp. 386–394.

[24] V. Kachitvichyanukul, "Comparison of three evolutionary algorithms: GA, PSO, and DE," *Ind. Eng. Manage. Syst.*, vol. 11, no. 3, pp. 215–223, Sep. 2012.

[25] V. Roberge, M. Tarbouchi, and G. Labonte, "Comparison of parallel genetic algorithm and particle swarm optimization for real-time UAV path planning," *IEEE Trans. Ind. Informat.*, vol. 9, no. 1, pp. 132–141, Feb. 2013.

[26] A. Deb, J. S. Roy, and B. Gupta, "Performance comparison of differential evolution, particle swarm optimization and genetic algorithm in the design of circularly polarized microstrip antennas," *IEEE Trans. Antennas Propag.*, vol. 62, no. 8, pp. 3920–3928, Aug. 2014.

[27] J.-P. Berenger, "A perfectly matched layer for the absorption of electromagnetic waves," *J. Comput. Phys.*, vol. 114, no. 2, pp. 185–200, Oct. 1994.

[28] M. Clemente, M. P. Fanti, G. Iacobellis, M. Nolich, and W. Ukovich, "A decision support system for user-based vehicle relocation in car sharing systems," *IEEE Trans. Syst., Man, Cybern. Syst.*, vol. 48, no. 8, pp. 1283–1296, Aug. 2018.

[29] R. Poli, J. Kennedy, and T. Blackwell, "Particle swarm optimization, an overview," *Swarm Intell.*, vol. 1, no. 1, pp. 33–57, 2007.

[30] Y. Shi and R. Eberhart, "A modified particle swarm optimizer," in *Proc. IEEE Int. Conf. Evol. Comput. World Congr. Comput. Intell.*, May 1998, pp. 69–73.

[31] R. Eberhart and Y. Shi, "Comparing inertia weights and constriction factors in particle swarm optimization," in *Proc. IEEE Congr. Evol. Comput.*, San Diego, CA, USA, Jul. 2000, pp. 84–88.

[32] *Road Traffic Noise Reducing Devices Test Method for Determining the Acoustic Performance—Part 3: Normalized Traffic Noise Spectrum*, Standard EN 1793-3:1997, European Committee for Standardization, 1997.

[33] *Road Traffic Noise Reducing Devices Test Method for Determining the Acoustic Performance—Part 6: Intrinsic Characteristics In situ Values of Airborne Sound Insulation Under Direct Sound Field Conditions*, Standard EN 1793-6:2018, European Committee for Standardization, 2018.

[34] V. Romero-García, J. V. Sánchez-Pérez, and L. M. Garcia-Raffi, "Tunable wideband bandstop acoustic filter based on two-dimensional multiphysical phenomena periodic systems," *J. Appl. Phys.*, vol. 110, no. 1, Jul. 2011, Art. no. 014904.

[35] *Road Traffic Noise Reducing Devices Test Method for Determining the Acoustic Performance—Part 6: Intrinsic Characteristics In Situ Values of Airborne Sound Insulation Under Direct Sound Field Conditions*, Standard EN 1793-6:2011, European Committee for Standardization, 2011.

[36] X. Blasco. (2022). *Basic Genetic Algorithm*. MATLAB Central File Exchange. Accessed: Nov. 22, 2022. [Online]. Available: https://www.mathworks.com/matlabcentral/fileexchange/39021-basic-genetic-algorithm

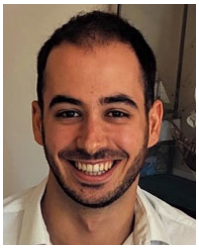

DAVID RAMÍREZ-SOLANA received the bachelor's degree in telecommunication engineering and the master's degree in acoustic from the Polytechnic University of Valencia (UPV). He is currently pursuing the dual Ph.D. degrees in applied physics with UPV and in electrical engineering with the Polytechnic University of Bari. His research interests include acoustic metamaterials and their optimization, using new algorithms and techniques. Also, he is interested in simulation numerical methods for acoustics and the automation of noise mitigation devices, including active noise control strategies.

JAVIER REDONDO received the bachelor's degree in physics from the Autonomous University of Madrid, in 1993, the Ph.D. degree from the Quantum and Nonlinear Optics Research Group, University of Valencia, and the Ph.D. degree in acoustics from the Polytechnic University of Valencia (UPV), in 2001. He was an Assistant Professor with UPV. He has been a Visiting Professor with Univesite du Maine, France, and McGill University, Canada. He is currently a Lecturer of acoustics with UPV. He is also the Director of the Master's Degree in Acoustic Engineering, UPV, and a Local Coordinator of the Erasmus Mundus Joint Master's Degree WAVES (Waves, Acoustics, Vibrations, Engineering and Sound). He is the coauthor of more than 40 articles in indexed scientific journals. His current research interests include simulation techniques in acoustics, room acoustics, building acoustics, metamaterials, and optimization using genetic algorithms.

AGOSTINO MARCELLO MANGINI (Senior Member, IEEE) received the Laurea degree in electronics engineering and the Ph.D. degree in electrical engineering from the Polytechnic University of Bari, Bari, Italy, in 2003 and 2008, respectively. He has been a Visiting Scholar with the University of Zaragoza, Zaragoza, Spain. He is currently an Associate Professor with the Department of Electrical and Information Engineering, Polytechnic University of Bari. He has authored or coauthored more than 90 printed publications. His current research interests include modeling, simulation, and control of discrete-event systems, Petri nets, supply chains and urban traffic networks, distribution and internal logistics, management of hazardous materials, management of drug distribution systems, and healthcare systems. He was on the Program Committees of the 2007–2015 IEEE International SMC Conference on Systems, Man, and Cybernetics and the 2009 IFAC Workshop on Dependable Control of Discrete Systems. He was on the editorial board of the 2017 IEEE Conference on Automation Science and Engineering.

MARIA PIA FANTI (Fellow, IEEE) received the Laurea degree in electronic engineering from the University of Pisa, Pisa, Italy, in 1983. Since 1983, she has been with the Department of Electrical and Information Engineering, Polytechnic University of Bari, Italy, where she is currently a Full Professor of system and control engineering and the Chair of the Laboratory of Automation and Control. She was a Visiting Researcher with the Rensselaer Polytechnic Institute, Troy, NY, USA, in 1999. Her research interest includes the management and modeling of complex systems, such as transportation, logistics, and manufacturing systems, discrete event systems, Petri nets, consensus protocols, and fault detection. She has published more than 315 articles and two textbooks on her research topics. She was a Member-at-Large of the Board of Governors of the IEEE Systems, Man, and Cybernetics Society. She is a member of the AdCom of the IEEE Robotics and Automation Society. She was the General Chair of the 2011 IEEE Conference on Automation Science and Engineering, the 2017 IEEE International Conference on Service Operations and Logistics, and Informatics, and the 2019 IEEE Systems, Man, and Cybernetics Conference. She is the Chair of the Technical Committee on Automation in Logistics of the IEEE Robotics and Automation Society. She was a Senior Editor of the IEEE TRANSACTIONS ON AUTOMATION SCIENCE AND ENGINEERING. She is an Associate Editor of the IEEE TRANSACTIONS ON SYSTEMS, MAN, AND CYBERNETICS: SYSTEMS.

Open Access funding provided by 'Politecnico di Bari' within the CRUI CARE Agreement